Gulf Journal of Mathematics ISSN: 2309-4966
Vol 17, Issue 2 (2024) 166-189 https://doi.org/10.56947/gjom.v17i2.1937

A GODUNOV-TYPE SCHEME FOR THE SAINT-VENANT-EXNER EQUATIONS WITH A MOVING STEADY STATES

SEYDOU SORE[1*], BABACAR LEYE[2] and YACOUBA SIMPORÉ[3]

Abstract. The Saint-Venant-Exner system is widely used in industrial codes to model the transport of bed sediments. In practice, most of the methods used for its numerical resolution suffer from significant stability problems due to the fact that they are mainly guaranteed by separation techniques which allow weak coupling between hydraulic and morphodynamic software. The search for an adequate alternative method to this problem is a focus towards which several approaches converge. Recently, many authors have proposed acceptable methods but they are not so trivial to implement in an industrial context and some do not take into account all aspects such as mobile steady states. In this work, we derive a well-balanced scheme that takes into account all stable states, to approach weak solutions of the sediment transport model in shallow waters. We demonstrate that it captures exactly all regular steady solutions with non-evanescent velocities, retains water level positivity and is able to degenerate to a classical shallow water model when the sedimentary transport flow is null. A number of numerical test cases are also presented to illustrate these properties.

1. Introduction

This study focuses on to the numerical approximation of solutions for the 1D nonlinear shallow water model coupled with a sedimentary continuity equation described by the Saint-Venant-Exner system. This system comprises three equations: the two equations of the shallow water flow model, which include source terms for topography and friction, and a simple conservation law that accounts for the interaction between the fluid and the topography.

$$\begin{cases} \partial_t h + \partial_x(hu) = 0, \qquad x \in \mathbb{R}, \quad t > 0 \\ \\ \partial_t hu + \partial_x\big(hu^2 + g\dfrac{h^2}{2}\big) = -gh(\partial_x b + T_f) \\ \\ (1-\phi)\partial_t b + \partial_x q_s = 0 \end{cases} \tag{1}$$

Date: Received: Apr 23, 2024; Accepted: Jul 7, 2024.

* Corresponding author.

2020 *Mathematics Subject Classification.* Primary 46L55; Secondary 44B20.

Key words and phrases. shallow-water equations, Exner equation, Godunov-type schemes, approximate Riemann solver, well-balanced scheme.

The unknowns of the problem are the water height $h(t, x) \geq 0$, the flow velocity $u(t, x)$ and $b(x)$, which defines the bottom topography. The parameters include the gravitational acceleration $g > 0$ and the porosity of the sedimentary layer ϕ, which will later be set to zero. We also introduce the fluid discharge $q(t, x) := h(t, x)u(t, x)$. The friction term T_f and the sediment flux q_s are fundamental elements of the model, because they ensure the coupling between the fluid and the solid parts.

During the two last decades, numerous works [15],[17],[27],[10],[28],[11],[14],[12], [13], [2],[3] have focused on developing numerical schemes to approximate the weak solutions of (1) and accurately capture the steady-state solutions. As noted in [15], if steady-state solutions are not properly captured, the approximation can result in significant errors over long time periods (see also [5] for an illustration). Since the ordinary differential equation defined by steady states, which we call ODE of steady states, turns out to be nonlinear, many works only consider the lake at rest steady states defined by the non-mobile steady states ($u = 0$ and a constant free surface $h + b$). With regard to the preservation of the balance of the lake at rest, many authors have developed numerical schemes preserving this balance [1],[6] and in particular, the reader is referred to the well-known hydrostatic reconstruction introduced by Audusse et al. [1] and the approximate Riemann Solver developed by Philippe Ung et al. [2]. It should be noted that the derivation of a schema capable of capturing all regular steady solutions is very difficult because the ODE of stable states can admit one, two or three solutions depending on the choice of constants. To our knowledge, so far no simple numerical scheme capable of capturing exactly this state has been developed in shallow waters with sedimentary transport. Regarding the transport of pollutants, Concerning the transport of pollutants, in [26] the authors, using deep neural networks informed by physics, carried out a perfect numerical simulation of the transport of pollutants in groundwater. For the classical shallow water model (Saint-Venant with fixed topography), in [15], the nonlinear system of ODEs for stable states is solved at each interface to develop a fully well-balanced scheme that can exactly capture all smooth steady solutions, both mobile and non-mobile. Subsequently, in [8], the authors proposed an extension of the hydrostatic reconstruction to address moving steady solutions. However, this generalized hydrostatic reconstruction does not preserve the positivity of the water height.

More recently, in [4], a Godunov scheme was derived to incorporate the source term within the approximate Riemann solver. This resulted in a positive, entropy-preserving scheme that exactly captures all smooth steady solutions. Unfortunately, this approach also requires solving a strongly nonlinear equation at each interface. Later, a numerical technique that captures all steady solutions exactly without solving the ODE of steady states was developed in [21]. This technique is based on a relevant linearization of the Godunov-type scheme to achieve a positive, fully well-balanced scheme. However, the topography source term introduces certain difficulties, as it is linked to a constant whose definition remains unresolved. The linearization adopted also introduces, in the definition of the numerical flux function, a disturbance necessary to recover the exact capture of steady states in motion which can in some cases be indefinite according to [5].

These limitations were overcome in [5] by adopting a new natural and consistent discretization of the source term and an improvement of the disturbance in order to obtain a well-defined numerical method. This technique was also adopted in [23] a well-defined Godunov-type scheme was derived for a Navier-Stokes model with a friction term. We are adopting this very attractive technique of Christophe Berthon et al. [4] which has been developed for the hyperbolic Saint-Venant equation, to extend it to the coupled solid transport and fluid flow system. This is how we obtain a numerical scheme capable of preserving all stable states for the case of sediment transport in shallow waters.

Another crucial aspect in designing numerical schemes for sediment transport in shallow waters is the technique of coupling the Saint-Venant and Exner equations to account for all interactions between the fluid and the solid components. Generally, the flow formula q_s causes the morphodynamic equation for b to be strongly coupled with the hydraulic part of the Saint-Venant-Exner model. Consequently, the model becomes highly nonlinear, making the eigenvalues and eigenvectors of the corresponding Jacobian flux matrix difficult to evaluate, and thus complicating the design of a straightforward coupled numerical approximation. Despite these challenges, most industrial codes [18],[19] rely on the Saint-Venant-Exner model for numerical simulations of sediment transport problems.

According to [2], the core of these software codes is the resolution of hydraulic problems (Saint-Venant). To address the sedimentary aspect, they employ sedimentary modules capable of solving the Exner equation. By doing so, both codes can operate with different numerical parameters such as time step, space step, or numerical scheme, and communicate only by exchanging specific data at certain time steps. This method of fractional division works well in certain cases but fails when dealing with rapid flow, introducing numerical instabilities [17]. In [2], this problem was addressed by numerically processing the complete Saint-Venant-Exner system with a semi-coupled approach. However, the treatment was done using a numerical scheme that preserves the lake-at-rest state rather than the general stationary states. In this work, we propose a similar approach, following the methods of Philippe Ung et al. [2], to extend the stabilization of the lake-at-rest state to equilibrium states in general (both mobile and non-mobile).

To achieve this, we adopt a Godunov-type scheme by proposing a positive and well-balanced three-wave Riemann solver capable of approximating the system (1) and degenerating into the well-balanced and positive solver introduced in [5] when the sedimentary flow is null (classical Saint-Venant equations). In this solver, we pay particular attention to the derivation of intermediate states that can be misdefined due to moving steady states. We use a coupled scheme for the complete model given by the system (1), which accounts for all stable states. This allows us to improve industrial codes by stabilizing the fractional approach and accurately capturing all steady solutions with non-evanescent speeds. We demonstrate that the designed scheme verifies the properties required by the Saint-Venant-Exner (1) system. Several numerical experiments are also presented to illustrate its relevance.

The document is structured as follows. Section 2 provides details about the Saint-Venant-Exner system (1). In Section 3, we design the Godunov-type scheme with a source term, which constitutes an appropriate definition of the approximate Riemann solver. Section 4 details the development of a relevant approximation of the source term for the approximate Riemann solver. Section 5 covers the complete derivation of the approximate Riemann solver. Section 6 presents the main properties satisfied by the derived scheme. Finally, in the last section, we present several numerical approximations to illustrate the relevance of the proposed scheme.

2. Description of the mathematical model

In this section, we give the friction term T_f and the sedimentary flux q_s that are necessary for the closure of the Saint-Venant-Exner system (1). We also discuss some properties of the Saint-Venant-Exner model that are necessary in the derivation of the numerical scheme.

2.1. Choice of formulas for friction term and sediment flux.

As mentioned earlier the friction term T_f is usually defined by semi-empirical formulas [2], in this paper we adopt the very popular Manning-Strickler formula,

$$T_f = \frac{|q|q}{K_s^2 h^2 R_h^{4/3}},$$

where $R_h \sim h$ is the hydraulic radius and K_s is a roughness coefficient.

As for the formula for the sediment flux q_s, we will use the formula of Lajeunesse et al. (2010) whose construction is detailed in [20] and defined by

$$q_s(t,x) = 10.6(\tau^* - \tau_c^*)(\sqrt{\tau^*} - \sqrt{\tau_c^*} + 0.025). \tag{2}$$

In this formula, τ^* denotes the Shields number (see [25]) which refers to a non-dimensional friction term that is weighted by the buoyancy of sediment particles. When it is larger than a cohesion, the particles then have a resistance to erosion greater than their weight.

$$\tau^* = \frac{\rho_w h T_f}{(\rho_s - \rho_w) D_{50}} \tag{3}$$

where ρ_w and ρ_s represent the densities of the aqueous phase and the solid phase, respectively, and D_{50} denotes the mean granular diameter.
τ_c^* is the critical Shields number (also called the dimensionless critical shear stress) that represents the minimum value of τ^* for solid transport to take place. Several works have been developed for its calculation [25], analyses by Shields (1936) have shown that its value must be a function of the Reynolds number and is close to 0.05.
We chose (2) because it is on the one hand a recent formula (2010) and on the other hand because this law has been tested and considered valid and reliable for different case studies, and takes into account the effects of relaxation. Indeed, CHARBI Mohamed, in [20], worked on simulation tests of the most used models in the calculation of sediment transport by cartage with experimental data from the literature and in order to verify the validity of this new model (2). A comparative study was carried out between the calculated results of these models for

the quantification of bottom transport and the corresponding experimental data. This study revealed the reliability of this new formula proposed by Lajeunessee et al. (2010).

2.2. **Properties of the Saint-Venant-Exner model.** To correctly approximate the solutions of the system (1), the numerical scheme must ensure the positivity of the height of the water and the well-balanced property particularly characterized here by the preservation of stationary states. The steady states of (1) without friction terms are defined by the ordinary differential equation

$$\begin{cases} \partial_x(hu) = 0, \\ \partial_x\big(hu^2 + g\dfrac{h^2}{2}\big) = -gh\partial_x b, \\ \partial_x q_s(h,u) = 0. \end{cases} \tag{4}$$

When the speed is zero, we obtain the fixed steady states usually called resting lake state defined as:

$$u = 0, \qquad \partial_x(h+b) = 0. \tag{5}$$

After direct calculations, the system (4) can be rewritten by showing the hydraulic head
$B(h,u,b) = u^2/2 + g(h+b)$ as follows:

$$\begin{cases} \partial_x(hu) = 0, \\ \partial_x\big(\dfrac{u^2}{2} + g(h+b)\big) = 0, \end{cases}$$

Consequently, for any given constant pair $(Q,B) \in \mathbb{R}^2$ regular stationary solutions are characterized by the following two relations:

$$.\begin{cases} hu = Q, \\ \dfrac{u^2}{2} + g(h+b) = B, \end{cases} \tag{6}$$

An important final property is the ability to revert to a scheme relevant to the classical shallow water model when sediment transport is null in the numerical model.

To simplify future notations, let us define

$$w = \begin{pmatrix} h \\ q \end{pmatrix}, \quad f(w,b) = \begin{pmatrix} q \\ \dfrac{q^2}{h} + \dfrac{gh^2}{2} \\ q_s \end{pmatrix}, \tag{7}$$

$$S_1(w,b) = \begin{pmatrix} 0 \\ -gh\partial_x b \\ 0 \end{pmatrix} \quad \text{and} \quad S_2(w,b) = \begin{pmatrix} 0 \\ -ghT_f \\ 0 \end{pmatrix}.$$

Additionally, we introduce the set of permissible physical states $\Omega \subset \mathbb{R}^2 \times \mathbb{R}$ defined as follows:

$$\Omega = \{(w, b) \in \mathbb{R}^2 \times \mathbb{R}; h > 0, u \in \mathbb{R}, b \in \mathbb{R}\}. \tag{8}$$

Thus the vector formulation of (1) is defined by

$$\partial_t (w, b)^T + \partial_x f(w, b) = S_1(w, b) + S_2(w, b). \tag{9}$$

3. Godunov-type schemes for the Saint-Venant-Exner model

We introduce a Godunov finite volume scheme for (1) when the friction term is neglected, its treatment will be described in section 5.5. Thus the system under consideration is

$$\partial_t (w, b)^T + \partial_x f(w, b) = S_1(w, b). \tag{10}$$

Consider a uniform mesh defined by the sequence of points $(x_{i+1/2})_{i\in\mathbb{Z}}$ such as, $x_{i+1/2} = x_{i-1/2} + \Delta x$, with Δx the step in assumed constant space. Thus, the space is divided into cells $C_i = (x_{i-1/2}, x_{i+1/2})$ centered in $x_i = x_{i-1/2} + \Delta x/2$.
In the same way, we define the sequence $(t^n)_{n\in\mathbb{N}}$ par $t^0 = 0$ and $t^{n+1} = t^n + \Delta t$, where Δt is the time step that must be restricted by a CFL condition.
We also adopt the ratings:

$$Y_L = \frac{1}{\Delta x}\int_{-\Delta x}^{0} Y(x)dx, \quad Y_R = \frac{1}{\Delta x}\int_{0}^{\Delta x} Y(x)dx \quad \text{and } Y_i = \frac{1}{\Delta x}\int_{C_i} Y(x)dx. \quad \forall Y \in \{h_0, q_0, b_0\}$$

At the time t^n, it is assumed to be known a constant approximation by pieces of the solution of (10) and defined as follows:

$$W_\Delta^n(x, t^n) = (w_i^n, b_i^n)^T \quad \text{if} \quad x \in C_i.$$

We are now looking for an updated approximation (w_i^{n+1}, b_i^{n+1}) of the solution at time $t^{n+1} = t^n + \Delta t$. For this we will solve the following problem:

$$\begin{cases} \partial_t (w, b)^T + \partial_x f(w, b) = S_1(w, b) \\ \\ \big(w^n(x, t^n), b^n(x, t^n)\big)^T = W_\Delta^n(x, t^n) \end{cases}$$

Locally, on each interface $x_{i+1/2}$, we are therefore led to consider a Riemann problem between two constant states associated with cells C_i and C_{i+1} defined by:

$$\begin{cases} \partial_t (w, b)^T + \partial_x f(w, b) = S_1(w, b) \\ \big(w^n(x, t^n), b^n(x, t^n)\big)^T = \begin{cases} (w_i^n, b_i^n)^T & \text{if} \quad x < 0 \\ \\ (w_i^n, b_{i+1}^n)^T & \text{if} \quad x > 0 \end{cases} \end{cases} \tag{11}$$

To achieve this, we first construct an approximate solution of the Riemann problem at each interface $x_{i+1/2}$, then we evaluate the average value of the juxtaposition of these solutions in each cell C_i at time t^{n+1} to obtain the new solution. Thus

$$(w_i^{n+1}, b_i^{n+1})^T = \frac{1}{\Delta x}\int_{C_i} W_\Delta^n(x, t^n + \Delta t)dx. \tag{12}$$

where $W^n_\Delta(x,t)$ represents the non-interaction juxtaposition of the approximate Riemann solvers defined on each cell $x_{i+1/2}$ as follows:

$$W^n_\Delta(x,t) = \tilde{W}_{\mathcal{R}}(\frac{x - x_{i+1/2}}{t}, w^n_i, w^n_{i+1}, b^n_i, b^n_{i+1}) \quad \text{if} \quad (x,t) \in (x_i, x_{i+1}) \times (0, \Delta t),$$

where, $\tilde{W}_{\mathcal{R}}(\frac{x}{t}; w_L, w_R, b_L, b_R)$ denotes an appropriate approximation of the solution of the Riemann problem defined by (11). According to [16],[5], the approximate Riemann solver must satisfy the following integral consistency condition:

$$\frac{1}{\Delta x}\int_{-\Delta/2}^{\Delta/2} \tilde{W}_{\mathcal{R}}(\frac{x}{t}, w_L, w_R, b_L, b_R)dx = \frac{1}{\Delta x}\int_{-\Delta/2}^{\Delta/2} W_R(\frac{x}{t}, w_L, w_R, b_L, b_R)dx, \quad (13)$$

where, $W_{\mathcal{R}}(\frac{x}{t}; w_L, w_R, b_L, b_R)$ is the exact solution of the Riemann problem defined by (11).

By approximation of this consistency condition (13) (See [5]), we obtain a finite volume type reformulation of (12) as follows :

$$\begin{aligned}(w^{n+1}_i, b^{n+1}_i)^T = (w^n_i, b^n_i)^T - \frac{\Delta t}{\Delta x}\big(F(w^n_i, w^n_{i+1}, b^n_i, b^n_{i+1}) - F(w^n_{i-1}, w^n_i, b^n_{i-1}, b^n_i)\big) \\ + \frac{\Delta t}{2}(\bar{S}_1(w^n_i, w^n_{i+1}, b_i, b_{i+1}) + \bar{S}_1(w^n_{i-1}, w^n_i, b_{i-1}, b_i)) \quad (14)\end{aligned}$$

with the given numerical numerical flux

$$F(w_L, w_R, b_L, b_R) = \frac{1}{2}\big(f(w_R, b_R)+f(w_L, b_L)\big)-\frac{\Delta x}{4\Delta t}((w_R, b_R)^T-(w_L, b_L)^T)+\frac{\Delta x}{2\Delta t}(J^+_{LR}-J^-_{LR}), \quad (15)$$

where

$$J^-_{LR} = \frac{1}{\Delta x}\int_{-\Delta x/2}^{0} \tilde{W}_{\mathcal{R}}(\frac{x}{\Delta t}w_L, w_R, b_L, b_R)dx \quad (16)$$

$$J^+_{LR} = \frac{1}{\Delta x}\int_{0}^{\Delta x/2} \tilde{W}_{\mathcal{R}}(\frac{x}{\Delta t}w_L, w_R, b_L, b_R)dx, \quad (17)$$

And $\bar{S}_1$ must be defined according to a consistent discretization of S_1.
Thus ends the presentation of the Godunov type schemes with the source term.
The following sections will characterize the approximate Riemann solver $\tilde{W}_{\mathcal{R}}(x/t; w_L, w_R, b_L, b_R)$ and approximate the source term $\bar{S}_1(w_L, w_R, b_L, b_R)$ in order to complete the complete derivation of the schema.

4. Discretization of the source term

The function $\bar{S}_1(w_L, w_R, b_L, b_R)$ is a local approximation on each interface of the source term that must be constructed in such a way as to allow the (14) schema to preserve stationary solutions. Since this is a local approximation, it is necessary to define stationary solutions interface by interface (see [5]).

Definition 4.1. *A solution is locally stationary if for all states (w_L, b_L) and (w_R, b_R), we have*

$$h_L u_L = h_R u_R, \quad B(w_L, b_L) = B(w_R, b_R) \quad (18)$$

where $B(w,b)$ is the Bernoulli function given by (6).

Now, $\bar{S}_1$ must be fixed in such a way that if (w_L, b_L) and (w_R, b_R) verify the local equilibrium (18), then the approximate Riemann solution $\tilde{W}_{\mathcal{R}}(x/\Delta t; w_L, w_R, b_L, b_R)$ remains stationary, i.e.

$$\tilde{W}_{\mathcal{R}}(x/\Delta t; w_L, w_R, b_L, b_R) = \begin{cases} (w_L, b_L)^T & \text{if} \quad x < 0 \\ \\ (w_R, b_R)^T & \text{if} \quad x > 0. \end{cases} \tag{19}$$

The relation (19) is used to propose a discretization of the source term using the condition of approximate integral consistency (13). Indeed, this condition for a stationary solution in the form (18), rewrites as follows:

$$\Delta x \bar{S}_1 = f(w_R, b_R) - f(w_L, b_L).$$

Since (w_L, b_L) and (w_R, b_R) are given according to (18), with $\bar{S}_1 = (\bar{S}_1^h, \bar{S}_1^q, \bar{S}_1^b)^T$, we have

$$\begin{aligned} &\Delta x \bar{S}_1^h = 0, \\ &\Delta x \bar{S}_1^q = (h_R u_R^2 + g\frac{h_R^2}{2}) - (h_L u_L^2 + g\frac{h_L^2}{2}), \\ &\Delta \bar{S}_1^b = 0. \end{aligned} \tag{20}$$

Since the equations for water height and bottom dimension do not include a source term, we set $\bar{S}_1^h = 0$ and $\bar{S}_1^b = 0$. Our focus is on $\bar{S}_1^q$, which we need to design to ensure a consistent definition of the topographic source term $-gh\partial_x b$. Additionally, we aim to validate equation (20) whenever (w_L, b_L) and (w_R, b_R) represent a local stable solution (18). To address this problem, we now establish a condition that $\bar{S}_1^q$ must satisfy (refer to [5], section 3).

Lemma 4.1. *Consider an approximation of the well-known Froude number defined given by*

$$\bar{F}_r^2 = \frac{q_0^2 \bar{h}}{g h_L^2 h_R^2}, \qquad \textit{where} \quad \bar{h} = \frac{1}{2}(h_L + h_R) \quad \textit{and} \quad q_0 = h_L u_L = h_R u_R. \tag{21}$$

If (w_L, b_L) and $w_R, b_R)$ are steady states according to (18), then the identity (20) is reformulated as follows:

$$\Delta x \bar{S}_1^q = \begin{cases} 0 \quad \textit{if} \quad \bar{F}_r = 1 \quad \textit{and} \quad \epsilon_{LR} = 0 \\ -g\bar{h}\Delta b + \dfrac{\bar{q^2}}{4h_L^2 h_R^2} \times \dfrac{h_R - h_L}{(1 - \bar{F}_r^2)^2 + \epsilon_{LR}\Delta x^k}(\Delta b)^2 \quad \textit{elsewhere,} \end{cases} \tag{22}$$

where $0 < k < \dfrac{3}{2}$ is a parameter to be set and

$$\bar{q^2} = |q_L q_R|, \qquad \epsilon_{LR} = \sqrt{|B(w_R, b_R) - B(w_L, b_L)| + |q_R - q_L|}. \tag{23}$$

5. Approximate Riemann solver

This section focuses on developing an appropriate approximate Riemann solver, $\tilde{W}_{\mathcal{R}}(x/t; w_L, w_R, b_L, b_R)$, to complete the characterization of the numerical scheme (14). This solver must be defined in accordance with the integral consistency condition (13), where the approximation of the source term $\bar{S}_1(w_L, w_R, b_L, b_R) = (0, \bar{S}_1^q, 0)^T$ is given by (22). Therefore, we consider an approximate Riemann solver consisting of three waves propagating with velocities $\lambda_L < 0$, $\lambda_0 = 0$, and $\lambda_R > 0$. In this case, the approximate Riemann solver, composed of two intermediate constant states (w_L^*, b_L^*) and (w_R^*, b_R^*), is defined as follows:

$$\tilde{W}_{\mathcal{R}}(x/t; w_L, w_R, b_L, b_R) = \begin{cases} (w_L, b_L) & \text{if } \quad \dfrac{x}{t} < \lambda_L \\ (w_L^*, b_L^*) & \text{if } \quad \lambda_L < \dfrac{x}{t} < 0 \\ (w_R^*, b_R^*) & \text{if } \quad 0 < \dfrac{x}{t} < \lambda_R \\ (w_R, b_R) & \text{if } \quad \dfrac{x}{t} > \lambda_R \end{cases} . \tag{24}$$

Note that the sentence Note that the determination of $\tilde{W}_{\mathcal{R}}$ is achieved once the two intermediate states (w_L^*, b_L^*) and (w_R^*, b_R^*) are defined. Unlike the Saint-Venant system discussed in [5], it is also necessary to define b_L^* and b_R^* since the bathymetry is mobile.

Such an approximate solver is consistent with (1) [7], [2], provided that the following consistency relations are satisfied by the intermediate states:

$$f(w_R, b_R) - f(w_L, b_L) = \lambda_L((w_L^*, b_L^*)^T - (w_L, b_L)^T) + \lambda_R((w_L, b_L)^T - (w_R^*, b_R^*)^T) + \bar{S}_1(w_L, w_R, b_L, b_R), \tag{25}$$

where $f(w, b)$ and $\bar{S}_1(w_L, w_R, b_L, b_R)$ are defined by (13) and (22), respectively. (25) translates to,

$$q_R - q_L = \lambda_L(h_L^* - h_L) + \lambda_R(h_R - h_R^*), \tag{26}$$

$$\lambda_L(q_L^* - q_L) + \lambda_R(q_R - q_R^*) = (h_R u_R^2 + \frac{g h_R^2}{2}) - \big(h_L u_L^2 + \frac{g h_L^2}{2}\big) + \Delta x \bar{S}_1^q. \tag{27}$$

$$q_s(w_R) - q_s(w_L) = \lambda_L(b_L^* - b_L) + \lambda_R(b_R - b_R^*) \tag{28}$$

Let's introduce the following notations to be simpler

$$h^{HLL} = \frac{\lambda_R h_R - \lambda_L h_L}{\lambda_R - \lambda_L} - \frac{q_R - q_L}{\lambda_R - \lambda_L} \tag{29}$$

$$q^{HLL} = \frac{\lambda_R h_R u_R - \lambda_L h_L u_L}{\lambda_R - \lambda_L} - \frac{1}{\lambda_R - \lambda_L}\big((h_R u_R^2 + \frac{g h_R^2}{2}) - (h_L u_L^2 + \frac{g h_L^2}{2})\big), \tag{30}$$

as defined, h^{HLL} and q^{HLL} are respectively the water height and intermediate discharge associated with the Solver HLL (Harten, Lax and van Leer) which is well known (see [7]).

Then, the relations (26), (27) and (28) are reformulated as follows:

$$\lambda_R h_R^* - \lambda_L h_L^* = (\lambda_R - \lambda_L) h^{HLL}, \tag{31}$$

$$\lambda_R q_R^* - \lambda_L q_L^* = (\lambda_R - \lambda_L) q^{HLL} + \Delta x \bar{S_1^q}, \tag{32}$$

$$q_s(w_R) - q_s(w_L) = \lambda_L(b_L^* - b_L) + \lambda_R(b_R - b_R^*). \tag{33}$$

To determine intermediate states, it is necessary to define six values. However, at this point we only have three equations (31), (32) and (33). It is therefore obvious that three relationships are missing.
On the one hand, we suggest imposing,

$$h_L^* u_L^* = h_R^* u_R^*, \tag{34}$$

$$u_L^{*2} + 2g(h_L^* + b_L^*) = u_R^{*2} + 2g(h_R^* + b_R^*) \tag{35}$$

These two relations that correspond to the definition of local steady state (18) are appropriate since we must also preserve stable states.

However, since (35) introduces significant nonlinearities (see [4] for such a choice with the Saint-Venant system), it is preferable to replace it with a relevant additional equation. Specifically, using $h_L^* = h_L$ and $h_R^* = h_R$ is the unique solution as long as (w_L, b_L) and (w_R, b_R) satisfy (18).

According to [21], this nonlinear system can be replaced by a linear system that retains all the necessary properties. In [21], for the case of Saint-Venant, the following additional relations are adopted:

$$h_R^* - h_L^* = \frac{\Delta x \bar{S_1^q}}{\alpha_{LR}}, \tag{36}$$

where

$$\alpha_{LR} = g\bar{h} - \frac{\overline{q^2}}{h_L h_R}, \quad \text{where} \quad \overline{q^2} \quad \text{is defined by} \quad (31). \tag{37}$$

Which was later improved in [5] to give (38), to take into account all solutions

$$h_R^* - h_L^* = \frac{\alpha_{LR} \Delta x \bar{S_1^q}}{\alpha_{LR}^2 + \epsilon_{LR} \Delta x^k}. \tag{38}$$

We extend this relevant reformulation to the case of Saint-Venant-Exner as follows:

$$h_R^* - h_L^* = \frac{\alpha_{LR} \Delta x \bar{S_1^{q*}}}{\alpha_{LR}^2 + \epsilon_{LR} \Delta x^k}. \tag{39}$$

where $\Delta x \bar{S_1^{q*}}$ is the approximation of the source term when (w_L, b_L) and (w_R, b_R) verify (18). On the other hand, to obtain the sixth relation, we adopt a minimization problem for the topography variable under the constraint given by the consistency relation (28) satisfied by this same variable, this problem was initially introduced in [2],

$$\min \mathcal{G}(b_L^*, b_R^*) = ||b_L - b_L^*||^2 + ||b_R - b_R^*||^2 \tag{40}$$

$$u.c. H(b_L^*, b_R^*) = \lambda_L(b_L^* - b_L) + \lambda_R(b_R - b_R^*) - (q_s(h_R, u_R) - q_s(h_L, u_L)) = 0.$$

Thus, the system of nonlinear relations (26)-(28), (35)-(39), and (40) allows us to explicitly determine the six intermediate states, as detailed in the following subsections. First, we easily explain the discharge, as it must remain constant to define a steady state. Next, we solve the minimization problem separately to determine the values of b_L^* and b_R^*. Finally, we use these values as input for the system (31)-(39), which is the same as the one discussed in [5]. However, the solution differs from that in [5] because, in this case, the bed elevation appearing in (39) is unknown and corresponds to an intermediate state to be determined.

5.1. **Expression of intermediate discharge.** It should be noted, to define a steady state, the discharge must be constant. Thus, by solving the equation (32) and adopting the following equalities with respect to the intermediate discharge,

$$q_L^* = q_R^* = q^*, \tag{41}$$

then the intermediate discharge is given by

$$q^* = q^{HLL} + \frac{\Delta x \bar{S}_1^q}{\lambda_R - \lambda_L}. \tag{42}$$

5.2. **Expression of the intermediate states of the solid part and the wave velocities λ_L and λ_R.** The expressions of the intermediate topography b_L^* and b_R^* is obtained through solving the minimization problem (40). Using the classical method of Lagrange multipliers, we adopt:

$$b_L^* = b_L + \frac{\lambda_L}{\lambda_L^2 + \lambda_R^2}\Delta q_s, \qquad b_R^* = b_R - \frac{\lambda_R}{\lambda_L^2 + \lambda_R^2}\Delta q_s. \tag{43}$$

The wave velocities in the model are determined by approximating the solutions of the characteristic polynomial of the Jacobian matrix $F'(W)$. Various techniques have been proposed in the literature, but most rely on strong assumptions about the polynomial coefficients. In this paper, we adopt the approach proposed in [2]. The authors in that study use Nickalls' technique [22], which involves differentiating the polynomial until a quadratic polynomial is obtained to find its solutions. Thus, the wave velocities used are (see [2]):

$$\lambda_L = \min_{w=w_L,w_R}\left(\frac{2u}{3} - \frac{2}{3}\sqrt{u^2 + gh(1+\beta)}, 0\right), \quad \lambda_R = \max_{w=w_L,w_R}\left(\frac{2u}{3} + \frac{2}{3}\sqrt{u^2 + gh(1+\beta)}, 0\right), \tag{44}$$

where

$$\alpha = \frac{\partial q_s}{\partial h}, \quad \beta = \frac{\partial q_s}{\partial q} \quad \text{and} \quad q = hu.$$

5.3. **Expression of the intermediate states of the hydraulic part.** To estimate intermediate water heights h_L^* and h_R^*, We solve the linear system (31)-(39) and the solution is directly given by

$$h_L^* = h^{HLL} - \frac{\lambda_R \alpha_{LR} \Delta x \bar{S}_1^{q*}}{(\lambda_R - \lambda_L)(\alpha_{LR}^2 + \epsilon_{LR}\Delta x^k)}, \tag{45}$$

$$h_R^* = h^{HLL} - \frac{\lambda_L \alpha_{LR} \Delta x \bar{S}_1^{q*}}{(\lambda_R - \lambda_L)(\alpha_{LR}^2 + \epsilon_{LR}\Delta x^k)}. \tag{46}$$

Unlike the case of shallow waters treated in [5], where the bathymetry is constant, here it is variable so we should define the term intermediate source.
For simplicity in the notation, let us introduce

$$\gamma_{LR} = \frac{\lambda_L + \lambda_R}{\lambda_L^2 + \lambda_R^2}$$

Using (43), we get,

$$(b_R^* - b_L^*)^2 = (b_R - b_L) - \gamma_{LR}\Delta q_s(2\Delta b - \gamma_{LR}\Delta q_s),$$

which makes it possible to obtain the expression of the intermediate source term

$$\Delta x \bar{S_1^{q*}} = \Delta x \bar{S_1^q} + \gamma_{LR} g \bar{h} \Delta q_s + \frac{\gamma_{LR}\Delta q_s \bar{q}^2}{4h_L^2 h_R^2} \times \frac{(h_R - h_L)(\gamma_{LR}\Delta q_s - 2\Delta b)}{(1 - \bar{F}_r^2)^2 + \epsilon_{LR}\Delta x^k} \tag{47}$$

However, this method of assessing intermediate water heights does not ensure that h_L^* and h_R^* remain positive. Therefore, we adopt a positive cut-off approach introduced in [4] (see also [5]). Accordingly, h_L^* and h_R^* are corrected as:

$$\tilde{h}_L^* = \min\big(\max\big(h_L^*, \sigma\big), (1 - \frac{\lambda_R}{\lambda_L})h^{HLL} + \frac{\lambda_R}{\lambda_L}\sigma\big), \tag{48}$$

$$\tilde{h}_R^* = \min\big(\max\big(h_R^*, \sigma\big), (1 - \frac{\lambda_L}{\lambda_R})h^{HLL} + \frac{\lambda_L}{\lambda_R}\sigma\big), \tag{49}$$

where $\sigma = \min(h_L, h_R, h^{HLL})$. It should be noted that as defined, the proposed reduction in water level not only satisfies positivity but preserves conservation since the relation (31), or equivalently (26), is always satisfactory. Indeed, note that as long as the exact height of the water height of the Riemann solution h_R remains positive, then $h^{HLL} > 0$ and by definition σ, we have the reduction $\sigma - h^{HLL} \leq 0$.
For positivity, since $\lambda_L < 0 < \lambda_R$ then we get

$$(1 - \frac{\lambda_R}{\lambda_L})h^{HLL} + \frac{\lambda_R}{\lambda_L}\sigma = h^{HLL} + \frac{\lambda_R}{\lambda_L}(\sigma - h^{HLL}) > 0, \tag{50}$$

$$(1 - \frac{\lambda_L}{\lambda_R})h^{HLL} + \frac{\lambda_L}{\lambda_R}\sigma = h^{HLL} + \frac{\lambda_L}{\lambda_R}(\sigma - h^{HLL}) > 0. \tag{51}$$

As a result, we immediately get $\tilde{h}_L^* > 0$ and $\tilde{h}_R^* > 0$.

5.4. **Discretization of the friction term.** The numerical treatment of the friction term is necessary to take into account the action of the solid part on the fluid. We adopt an implicit treatment that guarantees the stability of the schema that is presented in [2](see also[24]). q_i^{n+1} being the solution of (10) at time t^{n+1}, the solution of (1) (or (9)) $\tilde{q}_i^{n+1}$ at time t^{n+1} is given by

$$\tilde{q}_i^{n+1} = \begin{cases} \dfrac{-1 + \sqrt{1 + 4aq_i^{n+1}}}{2a}, & \text{if} \quad q_i^{n+1} > 0, \\ \\ \dfrac{1 - \sqrt{1 - 4aq_i^{n+1}}}{2a}, & \text{if} \quad q_i^{n+1} \leq 0, \end{cases} \tag{52}$$

with $a = \dfrac{g\Delta t}{K_s^2 h_i^{n+1}(R_{h,i}^{n+1})^{4/3}}$ Thus, the approximate Riemann solver (24) is now defined. To conclude this section, we establish that it preserves steady solutions and that it is capable of degenerating to an approximate Riemann solver for the Saint Venant case only.

Lemma 5.1. *Let (w_L, b_L) and (w_R, b_R) given in Ω. Consider the approximate Riemann solver as (24) where the intermediate states are given by (42), (48) and (49). If (w_L, b_L) and (w_R, b_R) satisfy the local equilibrium condition (18) with $\bar{F}_r \neq 1$, then the approximate Riemann solver remains at rest, namely that we have*

$$\tilde{W}_{\mathcal{R}}(x/\Delta t; w_L, w_R, b_L, b_R) = \begin{cases} (w_L, b_L)^T & \text{if} \quad x < 0 \\ \\ (w_R, b_R)^T & \text{if} \quad x > 0 \end{cases} \tag{53}$$

Proof The local equilibrium state (18) being satisfied, then $q_L = q_R = q_0$ and ϵ_{LR} is null through its definition (23), in this case,

$$\Delta x \bar{S}_1^q \frac{\alpha_{LR}}{\alpha_{LR}^2 + \epsilon_{LR}\Delta x^k} = \frac{\Delta x \bar{S}_1^q}{\alpha_{LR}} \quad \text{and} \quad h^{HLL} = \frac{\lambda_R h_R - \lambda_L h_L}{\lambda_R - \lambda_L},$$

Then (22) and (37) are used to establish

$$\frac{\Delta x \bar{S}_1^q}{\alpha_{LR}} = h_R - h_L,$$

and finally

$$h^{HLL} - \frac{\lambda_R}{\lambda_R - \lambda_L}\Delta x \bar{S}_1^q \frac{\alpha_{LR}}{\alpha_{LR}^2 + \epsilon_{LR}\Delta x^k} = h_L,$$
$$h^{HLL} - \frac{\lambda_L}{\lambda_R - \lambda_L}\Delta x \bar{S}_1^q \frac{\alpha_{LR}}{\alpha_{LR}^2 + \epsilon_{LR}\Delta x^k} = h_R,$$

Then according to (45) and (46), we easily get $h_L^* = h_L$ and $h_R^* = h_R$. With regard to the intermediate discharge, since the local equilibrium state (6) is verified, $\bar{S}_1^q$ is now given by (20) and we have the following equality:

$$\frac{\Delta x \bar{S}_1^q}{\lambda_R - \lambda_L} = \frac{(h_R u_R^2 + g\frac{h_R^2}{2}) - (h_L u_L^2 + g\frac{h_L^2}{2})}{\lambda_R - \lambda_L},$$

This allows, from (42), to obtain $q^* = q$ through simple calculations, then the discharge is stationary. There is now the intermediate bathymetry, since the local equilibrium state (6) is verified, (4) gives us $\Delta q_s = 0$, which makes it possible to obtain $b_L^* = b_L$ and $b_R^* = b_R$ through (43). Thus as soon as the state of equilibrium is reached then the solver remains at rest. □

Lemma 5.2. *Let (w_L, b_L) and (w_R, b_R) given in Ω. Consider the approximate Riemann solver as (24) where the intermediate states are given by (42), (48), (49), and (43). When the sediment flux is null in the Saint-Venant-Exner system*

$(q_s = 0)$, *the approximate Riemann solver then reduces to the case of the Saint-Venant system treated in* [5], *i.e. the dimension of the topographic background becomes fixed with respect to time.*

Proof For null sediment flux in the derived scheme, (43) gives us directly $b_L^* = b_L$ and $b_R^* = b_R$. Moreover, with (47), we get $\Delta x \bar{S_1^{q*}} = \Delta x \bar{S_1^q}$ and the intermediate water heights h_L^* and h_R^* given by (45) and (46) are now defined exactly as in the case of Saint-Venant discussed in [5]. Thus, the defined schema is degeneric. □

6. The main properties of the schema

Since the (14) scheme is now equipped with an approximate Riemann solver (24), where the intermediate states are given by (42), (48), (49) and (43) and a well-discretized source term (22), its design is complete. It satisfies the main properties below.

Theorem 6.1. *Suppose the CFL-Current-Friedrichs-Lewy type restriction* [9]

$$\Delta t \leq \frac{1}{2} \frac{\Delta x}{\max\limits_{i \in \mathbb{Z}} \left(|\lambda_{i+1/2}^L|, |\lambda_{i+1/2}^R| \right)}. \tag{54}$$

The numerical scheme (14) *is consistent with the scheme* (1) *and for all* $i \in \mathbb{Z}$, $(w_i^n, b_i^n)^T \in \Omega$, *The updated states* $(w_i^{n+1}, b_i^{n+1})^T$ *satisfy the following properties:*

1. *Preservation of positivity :* $h_i^{n+1} > 0$ *for all* $i \in \mathbb{Z}$,
2. ***Well-balanced property*** *(Conservation of all regular steady states):* $(w_i^{n+1}, b_i^{n+1})^T = (w_i^n, b_i^n)^T$ *for any* $i \in \mathbb{Z}$ *as soon as* $((w_i^n, b_i^n)^T)_{i \in \mathbb{Z}}$ *checks*

$$q_i^n = Q \quad \text{and} \quad \frac{(q_i^n)^2}{2(h_i^n)^2} + g(h_i^n + b_i) = B \quad \text{pour tout} \quad i \in \mathbb{Z}, \tag{55}$$

   for data constants Q *and* B *such that two successive states satisfy* (18).
3. *Degeneracy : if* $q_s^n = 0$ *then* $b_i^{n+1} = b_i^n$ *for all* $i \in \mathbb{Z}$, $\quad n \in \mathbb{N}$.

Proof First, we establish the consistency of the derived scheme (14). To address this, we observe that the CFL condition (54) ensures that the sequence of the approximate Riemann solver remains non-interacting. Then, with $w_L = w_R = w \in \Omega$, the equations (23) (29),(30) and (22) make it easy to get

$$h^{Hll} = \sigma = \bar{h} = h, \qquad q^{Hll} = q \tag{56}$$

$$\epsilon_{LR} = \sqrt{g|b_R - b_L|}, \quad \alpha_{LR} = gh - q^2/h^2, \quad \Delta \bar{S_1^q} = -gh(b_R - b_L) \tag{57}$$

Finally, we show the consistency of the numerical stream and the source term. As for the numerical stream, (15) gives us

$$F(w, w, b, b) = f(w, b) + \frac{\Delta x}{2\Delta t}(J_{LR}^+ - J_{LR}^-), \tag{58}$$

where J^+_{LR} and J^-_{LR} are defined by (16) and (17). Using the approximate Riemann solver as (24), through (58), we get

$$F(w,w,b,b) = f(w,b) + \frac{\lambda_R}{2}(w^*_R - w) + \frac{\lambda_L}{2}(w^*_L - w). \tag{59}$$

Using (56) and (57) in the definition of intermediate states (42), (45),(46) and (43), applying Δx to be small enough, we get

$$\begin{aligned}
q^* &= q - \frac{1}{\lambda_R - \lambda_L} gh(b_R - b_L),\\
h^*_L &= h + \frac{\lambda_R}{\lambda_R - \lambda_L}\frac{gh - q^2/h^2 gh}{(gh - q^2/h^2)^2 + \Delta x^k\sqrt{|b_R - b_L|}} gh(b_R - b_L),\\
h^*_R &= h + \frac{\lambda_L}{\lambda_R - \lambda_L}\frac{gh - q^2/h^2}{(gh - q^2/h^2)^2 + \Delta x^k\sqrt{|b_R - b_L|}} gh(b_R - b_L).
\end{aligned}$$

With these relation and for $b_R = b_L = b$, we directly obtain the expected consistency of the numeric stream as follows:

$$F(w,w,b,b) = f(w,b)$$

Then, regarding the consistency of the discrete source term, as soon as $w_L = w_R = w$, (22) gives us directly

$$\bar{S}^q_1(w,w,b_L,b_R) = -gh\frac{\Delta b}{\Delta x}.$$

With a survey function, set $b_L = b(x - \frac{\Delta x}{2})$ and $b_R = b(x + \frac{\Delta x}{2})$ in order to obtain

$$\lim_{\Delta x \to 0} \bar{S}^q_1(w,w,b_L,b_R) = -gh\partial_x b. \tag{60}$$

Thus the discrete source term is consistent and therefore the established numerical scheme (14) is consistent with the scheme (1)
With regard to the positive character of h^{n+1}_i, since the intermediate water height, defined by (48)-(49), involved in the approximate Riemann solver, is positive, then according to (12), h^{n+1}_i is nothing but the integral of the positive quantities. As a result, we get $h^{n+1}_i > 0$.
As for the well-balanced property, since $((w^{n+1}_i, b^{n+1}_i)^T)_{i\in\mathbb{Z}}$ checks (55), at each interface, the local stationary condition (18) is satisfied. As a result of lemma 5.1, all uninteracted Riemann approximate solutions are constant, so that we obtain

$$\tilde{W}_{\mathcal{R}}\left(\frac{x - x_{i+1/2}}{\Delta x}; (w^n_i, b^n_i)^T, w^n_{i+1}, b_i, b_{i+1}\right) = \begin{cases} (w^n_i, b^n_i)^T & \text{if} \quad x_{i+1/2} < 0,\\ (w^n_{i+1}, b^n_{i+1})^T & \text{if} \quad x_{i+1/2} > 0. \end{cases} \tag{61}$$

Thus, we have the following sequence of equality:

$$\begin{aligned}(w_i^{n+1}, b_i^{n+1})^T &= \frac{1}{\Delta x}\int_{x_{i-1/2}}^{x_i} \tilde{W}_{\mathcal{R}}\big(\frac{x - x_{i-1/2}}{\Delta x}; w_{i-1}^n, w_i^n, b_{i-1}^n, b_i^n\big)dx \\ &+ \frac{1}{\Delta x}\int_{x_i}^{x_{i+1/2}} \tilde{W}_{\mathcal{R}}\big(\frac{x - x_{i+1/2}}{\Delta x}; w_i^n, w_{i+1}^n, b_i^n, b_{i+1}^n\big)dx, \\ &= (w_i^n, b_i^n)^T.\end{aligned}$$

Thus the steady states are preserved so the scheme is well balanced. To finish the proof let us show to press the degeneration of the numerical scheme.
For a null sediment flux q_s^n, as a result of lemma 5.2 we have

$$b_L^{*n} = b_L^n \quad \text{and} \quad b_R^{*n} = b_R^n. \tag{62}$$

Using (62) in (16)-(17), the approximate solver (24) gives us $J_{i+1/2}^+ - J_{i+1/2}^- = 0$ at its third component, which immediately obtains the zero value at the third component of the numeric stream F defined by (15) then directly $b_i^{n+1} = b_i^n$ using (14). □

7. Numerical simulation

To illustrate the behavior of the proposed scheme, which we will refer to as the Fully Well-Balanced Corrected Scheme with Nickalls (FWBCN), we perform several numerical experiments using a series of classic test cases from the literature, extending them to cover additional flow regimes. We study the simulation of the evolution of dunes in both fluvial and torrential flow regimes, as well as the dam-break failure problem on a movable bed with a dry state. For some test cases, we compare our results with those obtained by the well-known SimSol scheme [2], which has already been judged superior to three other methods.
As long as the exact solution is known, the behavior of the obtained approximate solutions is exhibited by evaluating the L^1, L^2 and L^∞ errors. We used the exact solutions proposed in [17],[27]

7.1. **Comparison of the scheme with another scheme in the evolution of dunes in a fluvial flow.** Here we compare our scheme results with those obtained by the well-known SimSol scheme whose results have already been judged to be better compared to those given by three other methods [2]. Thus, we consider the classic test case of the sediment transport problem which considers a hump under a fluvial flow. The length of the channel is $L = 1000m$ and the initial data is parameterized by,

$$\begin{cases} b(0,x) = \begin{cases} 0.1 + \sin^2\big(\dfrac{(x-300)\pi}{200}\big), & 300 \leqslant x \leqslant 500m \\ 0.1, & elsewhere, \end{cases} \\ h(0,x) = 10 - b(0,x), \\ u(0,x) = \dfrac{q_0}{h(0,x)}, \end{cases} \tag{63}$$

with $q(t,0) = q^0 = 10m^2/s$ the incoming flow. With a discretization of 2000 cells for domain, the figureb1 show us the the bottom topography at time $t = 750s$. The excellent performance of the numerical solution is highlighted in Table 1, where the numerical errors are presented. It appears that the scheme presented is the most accurate

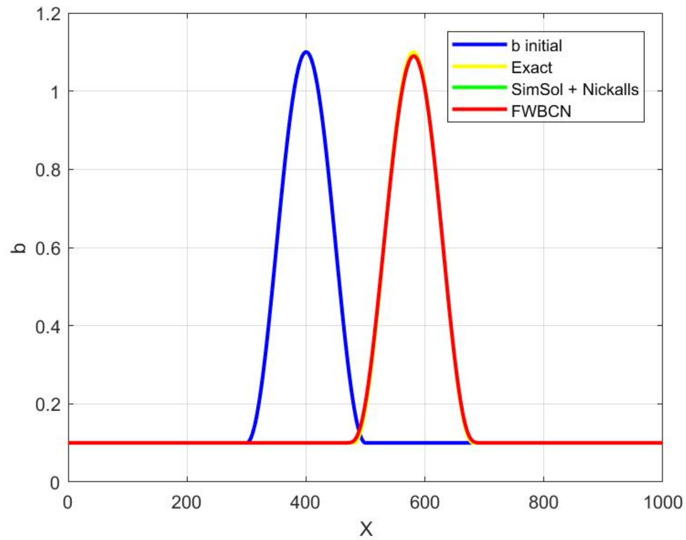

FIGURE 1. Comparison of dune evolution for different numerical schemes at $t = 750s$ with 2000s cell .

	b		
	L^1_{error}	L^2_{error}	L^∞_{error}
SimSol+Nickalls	0.0014	0.0036	0.0144
FWBCN	0.0013	0.0034	0.0139

TABLE 1. Dune evolution errors.

7.2. **Illustration of the benefits of using of the sediment flux formula.** Here we analyze the evolution of sediment transport calculated by different sediment flux formula. This test is used to see the benefits of using the sediment flux formula of Lajeunesse. We simulated problem (63) with the FWBCN-schema using the Lajeunesse formula and the Grass formula $q_s(t,x) = A_g|u|^{m-1}u$ with $m = 3$ and $A_g = 0.001$. The numerical simulations obtained at time $t = 550s$ are displayed Figure 2 and the obtained errors for b are given in Table 2

7.3. **Behavior of scheme when the sediment flux is null.** This test is used to analize the schema behaver when the sediment flux is null in the Saint-Venant-Exner system ($q_s = 0$). The expected result should be similar to one of a Saint-Venant schema treated in [5]. We consider the test probem in subcritical flow

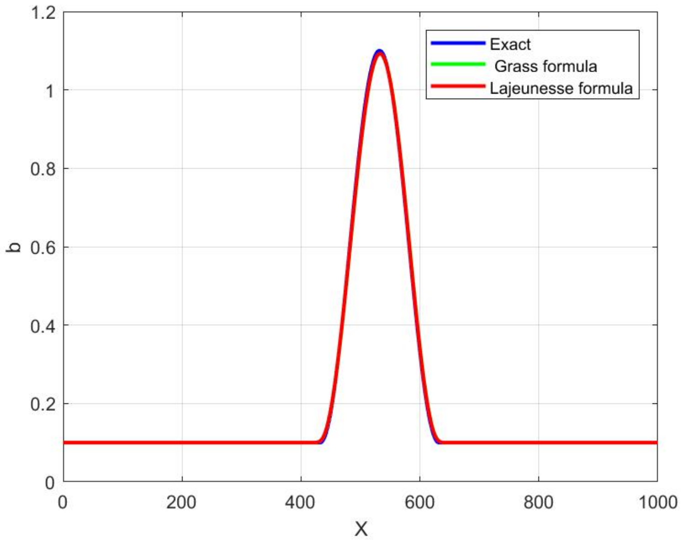

FIGURE 2. Comparison of the different formula at $t = 550s$ with 2000 cells.

	b+h		
	L^1_{error}	L^2_{error}	L^∞_{error}
FWBCN(Grass formula)	0.0016	0.0040	0.0150
FWBCN(Lajeunesse formula)	0.0013	0.0031	0.0122

TABLE 2. Free surface errors for different sediment flux formula.

that the domain is $[0, 25]$ and the initial data is given by,

$$\begin{cases} b(0,x) = max\big(0, 0.2 - 0.05(x-10)^2\big), \\ h(0,x) = 2m, \\ q(0,x) = 4.42m^2/2. \end{cases} \tag{64}$$

In figure 3 we show the numerical solution obtained with the different schemes at time $t = 64s$ with 2000 cells for domain discretization. Following the errors sumed up in the table 3, we can clearly see that the schema FWBCN completetly moves towards the schema FWBC.

	b+h		
	L^1_{error}	L^2_{error}	L^∞_{error}
FWBC & FWBCN	0.0000	0.0000	0.0000

TABLE 3. Free surface errors for for different schema with null sediment flux formula.

7.4. **Illustration of the ability of the scheme to capture steady states.** Here a test problem is used to illustrate the schema's ability to capture steady

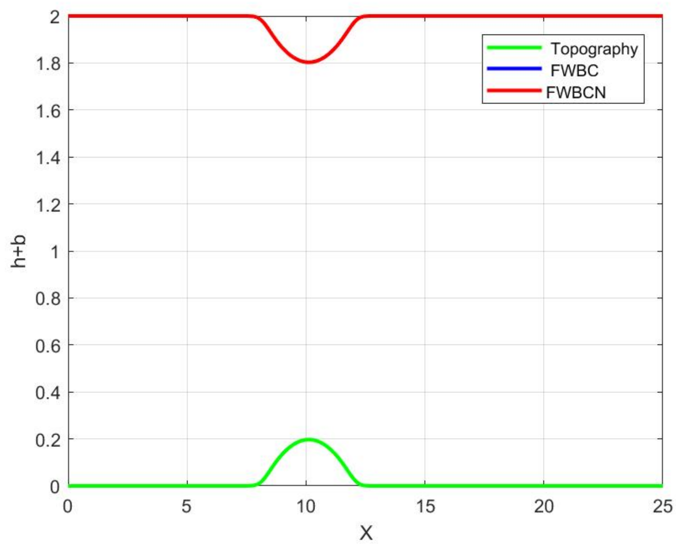

FIGURE 3. Comparison of free surface and the bottom topography evolution for different numerical schemes at $t = 64s$ with 2000 cells and $q_s(t, x) = 0$.

states. We consider the test probem in torrential flow that the domain is $[0, 25]$ and the initial data is given by,

$$\begin{cases} b(0,x) = max\big(0, 0.2 - 0.05(x-10)^2\big), \\ h(0,x) = 0.5m, \\ q(0,x) = 2m^2/2. \end{cases} \tag{65}$$

We evaluate the corresponding water height in the stationary state for the Bernoulli's law (6) with $Q = 2$ and $B = 12.905$,

$$\begin{cases} q(t,x) = Q, \\ \\ \dfrac{u^2}{2} + g(h+b) = B \end{cases} \tag{66}$$

First, the domain is discretized with 1000 cells and at time $t = 3.5s$ we compare the evolution results for different numerical schemes. The approximate solutions of the problem are presented in the figure 4. The excellent performance of the numerical solution is highlighted in Table 4, where the numerical errors are presented. by Table 4 where the numerical errors are given.Then we zoom on the result obtained with the FWBNC-scheme the to show the capture of the steady states. The result are presented in the figure 5 In this figure, it is clear that the approximate solution given by the schemes (FWBCN) is in very good agreement with reality. Indeed the scheme (FWBCN) preserves exactly such stationary solutions.

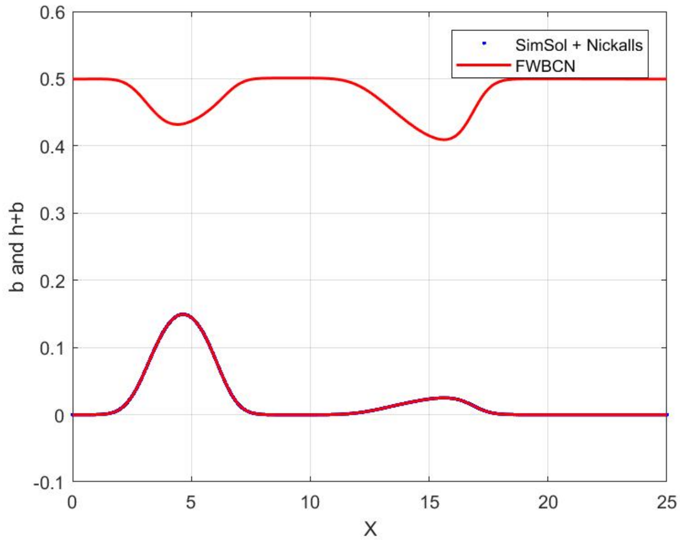

FIGURE 4. Free surface and dune evolution for different numerical schemes at $t = 3.5s$ with 1000 cells.

	b+h		
	L^1_{error}	L^2_{error}	L^∞_{error}
SimSol+Nickalls	$0.0060e^{-3}$	$0.0300e^{-3}$	$6.0000e^{-3}$
FWBCN	$0.0024e^{-4}$	$0.0120\ e^{-4}$	$2.3985e^{-4}$

TABLE 4. Free surface errors for for different schema for the schema's ability to capture steady states test.

7.5. **Dam break over a dry bottom topography.** This numerical simulation demonstrates the scheme's ability to accurately locate and process the dry/wet transition. We focus on this dam break problem as it is the most challenging transition situation. The domain is $[0, 20]$ with a topography flat. The initial height of the water is defined by

$$h(0,x) = \begin{cases} 2m, & \text{if} \quad x \leqslant 10, \\ 0m, & \text{if} \quad x > 10, \end{cases} \tag{67}$$

The domain is discretized into 500 cells, and the approximate solutions at different times are displayed in Figure 6. In Tables 5, we present the obtained errors for h+b at t = 0.5s. As with the previous test case, the FWCN scheme manages to solve the physical phenomenon since there is no instability.

	b+h		
	L^1_{error}	L^2_{error}	L^∞_{error}
FWBCN	$0.0153e^{-4}$	$0.0199e^{-4}$	$0.2803e^{-3}$

TABLE 5. Free surface errors for the dam-break on a dry domain.

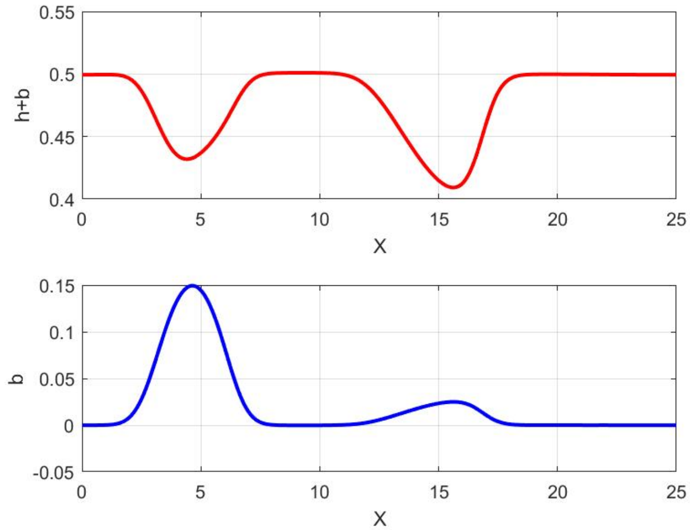

FIGURE 5. Free surface (up) and dune evolution (bottom) in a subcritical flow at $t = 3.5s$ with 1000 cells

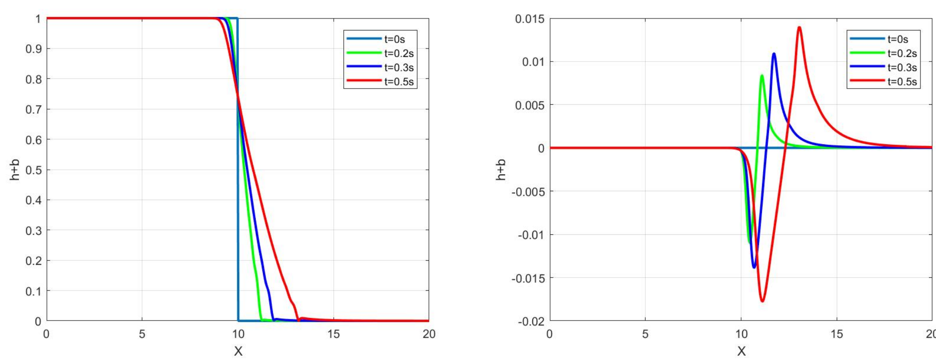

FIGURE 6. Simulation of the dam break over a dry bottom topography for t = 0 to 0.5s with 500 cells.

8. CONCLUSION

In this paper, we extend the approach developed by Christophe Berthon et al. for the hyperbolic Saint-Venant equation to the coupled solid transport and fluid flow system, following the methods of Philippe Ung et al. We propose a Godunov-type method based on a new approximate Riemann solver for the sediment transport system in shallow waters. This scheme, which avoids using an approximate Jacobian matrix of the system, is positive and well-balanced for all steady-state conditions. It has been successfully tested on two numerical test cases, making it the first simple approach with demonstrated stability properties for both mobile and non-mobile steady states.

References

[1] E. Audusse, F. Bouchut, M.-O. Bristeau, R. Klein, and B. Perthame. A fast and stable well-balanced scheme with hydrostatic reconstruction for shallow water flows. SIAM J. Sci. Comp., 25: 2050-2065, 2004. https://doi.org/10.1137/S1064827503431090

[2] Emmanuel Audusse, Christophe Chalons, Philippe Ung. A simple three-wave approximate Riemann solver for the Saint-Venant-Exner equations. International Journal for Numerical Methods in Fluids, 2018, 87 (10), pp.508-528. https://dx.doi.org/10.1002/fld.4500

[3] Barzgaran, M., Mahdizadeh, H., & Sharifi, S. (2019). Numerical simulation of bedload sediment transport with the ability to model wet/dry interfaces using an augmented Riemann solver. Journal of Hydroinformatics. https://doi.org/10.2166/HYDRO.2019.046

[4] C. Berthon and C. Chalons. A fully well-balanced, positive and entropysatisfying godunov-type method for the shallow-water equations. Mathematics of Computation, 85(299): 1281-1307, 2016. https://doi.org/10.1090/mcom3045

[5] Christophe Berthon, Meissa M'Baye, Minh H. Le, Diaraf Seck. A well-defined moving steady states capturing Godunov-type scheme for Shallow-water model. International Journal on Finite Volumes, 2020, 15. https://hal.science/hal-03192954v1

[6] Bollermann, A., Noelle, S., & Medvidov'a, M.L. (2011). Finite Volume Evolution Galerkin Methods for the Shallow Water Equations with Dry Beds. arXiv: Numerical Analysis, 371-404. https://doi.org/10.48550/arXiv.1501.03628

[7] F. Bouchut. Nonlinear stability of finite volume methods for hyperbolic conservation laws and well-balanced schemes for sources. Birkhäuser Verlag, Frontiers in Mathematics,2004. http://dx.doi.org/10.1007/b93802

[8] Castro, M.J., Milan, P., & Par, C. (2007). WELL-BALANCED NUMERICAL SCHEMES BASED ON A GENERALIZED HYDROSTATIC RECONSTRUCTION TECHNIQUE. Mathematical Models and Methods in Applied Sciences, 17, 2055-2113. http://dx.doi.org/10.1142/S021820250700256X

[9] Courant, R., Friedrichs, K., & Lewy, H. (1928). Über die partiellen Differenzengleichungen der mathematischen Physik. Mathematische Annalen, 100, 32-74. https://doi.org/10.1007/BF01448839

[10] Benkhaldoun, F., Sahmim, S., & Seaïd, M. (2009). Solution of the Sediment Transport Equations Using a Finite Volume Method Based on Sign Matrix. SIAM J. Sci. Comput., 31, 2866-2889. https://doi.org/10.1137/080727634

[11] Fayssal Benkhaldoun, Slah Sahmim, Mohammed Seaïd, A two-dimensional finite volume morphodynamic model on unstructured triangular, International Journal for numeriques methods in fluids 63, 11, 1296-1327, 2010. https://doi.org/10.1002/fld.2129

[12] Benkhaldoun, F., Seaid, M., & Sahmim, S. (2011). Mathematical Development and Verification of a Finite Volume Model for Morphodynamic Flow Applications. Advances in Applied Mathematics and Mechanics, 3, 470-492. https://doi:10.4208/aamm.10-m1056

[13] Benkhaldoun, F., Daoudi, S., Elmahi, I., & Seaïd, M. (2011). Comparison of unstructured finite-volume morphodynamic models in contracting channel flows. Math. Comput. Simul., 81, 2087-2097. https://doi.org/10.1016/j.matcom.2010.12.031

[14] E. D. Fernández-Nieto , C. Lucas, and J. Zabsonré. An energetically consistent viscous sedimentation model. Math. Models Methods Appl. Sci., 19(3): 477-499, 2009. http://dx.doi.org/10.1142/S0218202509003504

[15] L. Gosse. A well-balanced flux-vector splitting scheme designed for hyperbolic systems of conservation laws with source terms. Computers & Mathematics with Applications, 39(9):135-159, 2000. https://doi.org/10.1016/S0898-1221(00)00093-6

[16] A. Harten, P.D. Lax, and B. Van Leer. On upstream differencing and Godunovtype schemes for hyperbolic conservation laws. SIAM review, 25: 35-61, 1983. https://doi.org/10.1007/978-3-642-60543-7_4

[17] J. Hudson and P. K. Sweby. Formulations for numerically approximating hyperbolic systems governing sediment transport. J. Sci. Comput., 19: 225-252, 2003. http://dx.doi.org/10.1023/A:1025304008907

[18] Logiciel DELFT3D. . http://oss.deltares.nl/web/delft3d

[19] Logiciel HEC-RAS. . http://www.hec.usace.army.mil/software/hec-ras

[20] Mohamed Gharbi. Etudes des crues et du transport sédimentaire associé - Application au bassin versant de la Medjerda. Sciences de la Terre. Institut National Polytechnique de Toulouse - INPT; Institut national de la recherche agronomique (Tunisie), 2016. Français. https://www.theses.fr/2016INPT0008

[21] V. Michel-Dansac, C. Berthon, S. Clain, and F. Foucher. A well-balanced scheme for the shallow-water equations with topography. Computers & Mathematics with Applications, 72(3): 568-593, 2016. https://doi.org/10.1016/j.camwa.2016.05.015

[22] R. W. D. Nickalls. A new bound for polynomials when all roots are real. The Mathematical Gazette, 95(534): 520-526, November 2011. https://doi:10.1017/S0025557200003685

[23] Ouya, J., & Ouedraogo, A. (2024). A well-defined Godunov-type scheme in a Navier-Stokes model with a friction term. Gulf Journal of Mathematics, 16(2), 213-231. https://doi.org/10.56947/gjom.v16i2.1882

[24] A. Paquier. Modélisation et simulation de la propagation de l'onde de rupture de barrage. PhD thesis, Université Jean Monnet, October 1995. https://hal.inrae.fr/tel-02582031

[25] Shields, A. F. (1936). Application of similarity principles and turbulence research to bedload movement. Mitteilungen der preussischen versuchsanstalt fur wasserbau und schiffbau, Germany. pp. 5-24. https://api.semanticscholar.org/CorpusID:107385914

[26] Souleymane, Z., Bernard Lamien, Mohamed Beidari, & Tougri Inoussa. (2024). Numerical simulation of pollutants transport in groundwater using deep neural networks informed by physics. Gulf Journal of Mathematics, 16(2), 337-352. https://doi.org/10.56947/gjom.v16i2.1863

[27] Xin Wen, A steady state capturing and preserving method for computing hyperbolic systems with geometrical source terms having concentrations, Journal of Computational Physics 219 (2006) 322–390. https://doi.org/10.1016/j.jcp.2006.03.019

[28] J. Zabsonré, C. Lucas, and E. D. Fernández-Nieto. An energetically consistent viscous sedimentation model. Math. Models Methods Appl. Sci., 19(3): 477-499, 2009. http://dx.doi.org/10.1142/S0218202509003504

[1] Laboratoire LAMI, Université Norbert ZONGO, BP 376, Koudougou, Burkina Faso

Email address: seydousore27@gmail.com

[2] International Institute for Water and Environmental Engineering (2iE), BP 594 Ouagadougou 01, Burkina Faso

Email address: babacar.leye@2ie-edu.org

[3] Laboratoire LAMI, Université Norbert ZONGO, BP 376, Koudougou, Burkina Faso

Email address: simplesaint@gmail.com